A 280 GHz InP HBT Direct-Conversion Receiver with 10.8 dB NF

Utku Soylu[#1], Amirreza Alizadeh[#], Munkyo Seo[*], and Mark J. W. Rodwell[#]
[#]Department of Electrical and Computer Engineering, University of California, Santa Barbara, USA
[*]Department of Electrical and Computer Engineering, Sungkyunkwan University, South Korea
[1]utkusoylu@ucsb.edu

***Abstract*— We report a fully integrated 280 GHz direct-conversion receiver in 250 nm InP HBT technology. The receiver has > 17 dB conversion gain over 264-297 GHz, consumes 455 mW, and has 10.8-11.6 dB DSB noise figure over 261-300 GHz. Its –3 dB bandwidth is 16.5 GHz, while its –6 dB bandwidth is 34.5 GHz. The local oscillator is generated by an internal 8:1 active frequency multiplier. To the authors' knowledge, the IC demonstrates record noise performance for an integrated receiver operating near 280 GHz.**

***Keywords*—H-band, millimeter wave, direct conversion, noise figure (NF), indium phosphide (InP), double heterojunction bipolar transistor (DHBT).**

I. Introduction

The 200-300 GHz frequency range can support wireless backhaul links with capacities well above 100 Gb/s, serving future communications networks. Integrated receivers operating near 280 GHz have been demonstrated [1-9] in several technologies. Key design objectives for such receivers are low noise figure for increased link range and high bandwidth for high symbol rate hence high data rate. Here we report an integrated receiver with a 10.8-11.6 dB double sideband (DSB) noise figure over 261-300 GHz, record for receivers operating near 280 GHz. The receiver –3 dB bandwidth is 16.5 GHz, while its –6 dB bandwidth is 34.5 GHz. With moderate post-equalization, this bandwidth should be sufficient to support 50 GSymbol/second data transmission.

II. Receiver Design

The receiver was fabricated in Teledyne 250 nm InP HBT technology [10], this having a maximum 650 GHz power gain cut-off frequency (f_{max}) at top metal, a maximum 3 mA/μm current density, and 4.5 V BV_{CEO}. The technology provides four Au interconnect layers, 50 Ω/square thin film resistors, and 0.3 fF/μm^2 MIM capacitors.

The receiver has a broadband mm-wave low-noise amplifier, followed by down conversion mixers and broadband 50 Ω baseband output amplifiers for the in-phase (I) and quadrature-phase (Q) signals (Fig. 1). The mixers' local oscillators are generated by an 8:1 LO frequency multiplier, an LO buffer amplifier, and a passive LO quadrature phase generation circuit. In the LNA and frequency multiplier, IC interconnects are microstrip lines (MSL's) using the lowest

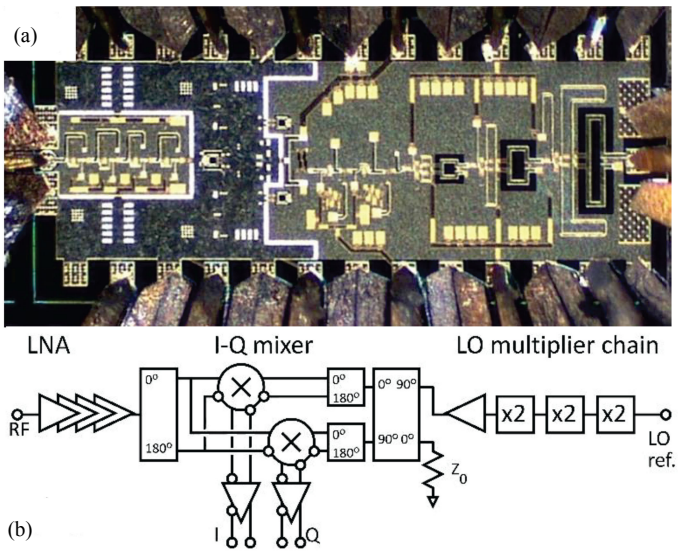

Fig. 1. 280 GHz direct-conversion receiver: integrated circuit photograph (a), and block diagram (b). The IC is 2.0 mm × 0.8 mm.

metal plane (M1) for ground. This provides lowest loss, hence best LNA noise figure. For the mixer and baseband amplifiers, the interconnects are inverted microstrip lines (IMSL's), using the upper (M4) metal plane for ground. IMSL does not require holes in the ground plane where each transistor is placed. This minimizes ground-return parasitics in dense circuits having many transistors, such as (I, Q) Gilbert-cell mixers. At 280 GHz, 50 Ω MSL loss is 1 dB/mm while IMSL loss is 1.9 dB/mm. The simulated MSL to IMSL transition loss is < 0.15 dB.

A. LO Multiplier (x8)

The 280 GHz LO is generated from a 35 GHz input using three cascaded frequency doublers (Fig. 2a); the multiplier chain was earlier reported in [11]. Each balanced frequency doubler cell uses a push-push emitter-coupled pair. The chain has an input transformer balun. At 280 GHz, the measured 8th harmonic power is –0.6 dBm. With –2 dBm input power, the multiplier 3-dB bandwidth is 48 GHz. Adjacent harmonics are suppressed by better than 28 dBc; given the LNA's finite RF bandwidth, other LO harmonics will not result in significant receiver spurious responses.

2023 IEEE Radio Frequency Integrated Circuits Symposium (RFIC) | 979-8-3503-2122-7/23/$31.00 ©2023 IEEE | DOI: 10.1109/RFIC54547.2023.10186196

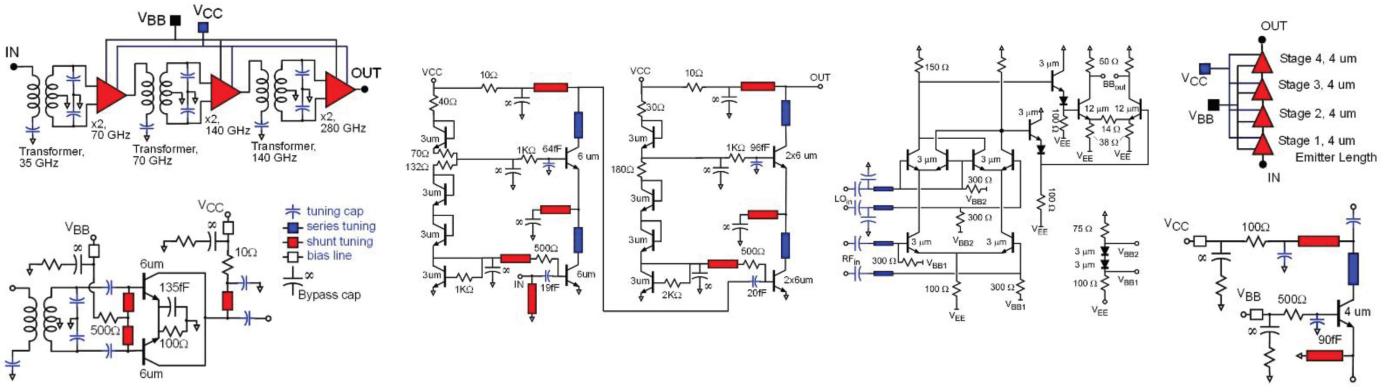

(a) (b) (c) (d)

Fig. 2. Circuit schematics: (a) LO Multiplier (×8), (b) LO Driver, (c) Mixer and 50-ohm Baseband Driver, (d) LNA

B. LO Driver

The driver amplifier increases the LO power to that necessary to drive the mixers. Though the DC bias circuit (Fig. 2b) is that of a pair of cascode stages, to provide highest output power and PAE there is impedance tuning between the outputs of the common-emitter (CE) and the inputs of the common-base (CB) transistors. The LO buffer amplifier is therefore best viewed as a four-stage (CE, CB, CE, CB) cascade. All inter-stage impedance tuning is for maximum saturated output power, given 0 dBm input power, not maximum small-signal gain. CE and CB transistors are individually stabilized, with the 500 Ω shunt resistors stabilizing the CE transistors and the finite base capacitance stabilizing the CB transistors. The finite base capacitance also provides significant cascade power-combining between the CB and CE stages [12, 13]. In simulation, given 0 dBm input power, the output power is > 7 dBm over 240-340 GHz. The simulated DC power is 160 mW.

C. I-Q Mixer and 50-Ohm Baseband Driver

The LO driver amplifier output feeds a Lange coupler and a pair of transformer baluns, generating the four (0°, 90°, 180°, 270°) LO phases required for the I and Q mixers. Each mixer is double-balanced in the Gilbert configuration (Fig. 2c), with impedance-matching on the LO and RF ports. There is no impedance matching between the input RF and LO switching transistors. Increasing the baseband load resistance from 50 Ω to 150 Ω reduces the noise contributions of the resistor itself and of the output buffer. The differential output amplifiers, with emitter followers as level-shifters and emitter degeneration for linearity, directly drives an external 50 Ω load. Simulated I-Q imbalance is < 0.4 dB in amplitude and < 7.8° in phase for DC-20 GHz output frequencies, including layout parasitics of Lange coupler, LO/RF transformers and the baseband output amplifier drivers.

D. LNA

The LNA (Fig. 2d) is a four-stage CB amplifier with base capacitive degeneration [12, 13, 14]. The base capacitance provides unconditional stability from DC to f_{max} and adjusts the source impedance for minimum noise measure to be the complex conjugate of the input impedance, allowing simultaneous input matching for reflection coefficient and for minimum cascaded noise figure. The HBT junction area is scaled, together with the DC current and the base capacitance, so that the source conductance for minimum noise measure is 20 mS; this permits the input stage to be noise-matched to 50 Ω with a single inductive shunt element, avoiding the added attenuation, hence the added noise, of a series matching element [14]. Center frequencies of the four stages are stagger-tuned to provide wider bandwidth.

III. Measurement Results

Measurements (Fig. 3) were performed on 3-mil thinned die (Fig. 1). A synthesizer and cascaded 12:1 and 2:1 VDI frequency multipliers generated the input signal, which passed through a directional coupler and a 220-330 GHz GGB wafer probe. The coupler −20 dB port, connected to a harmonic mixer and spectrum analyzer, monitored the input power; before IC testing, this input power monitor was calibrated against a VDI/Erickson THz power meter. The receiver output power was measured by a power meter and its spectrum monitored by a spectrum analyzer. Measurements are corrected for the input probe loss using the loss stated on the probe data sheet.

In operation, the 8:1 multiplier was biased with V_{CC}=2.9 V and V_{BB}=1.9 V, drawing 29.8 mA and 1.2 mA respectively. The 4-stage LNA was biased with V_{CC} =1.6 V and V_{BB} =0.85 V, drawing 11 mA and 0.51 mA respectively. The LO driver was biased with V_{CC} =4.7 V, and drew 31 mA from this supply. The mixers and output buffers drew 81 mA from V_{EE} = –2.5 V. The DC power dissipation is 455 mW.

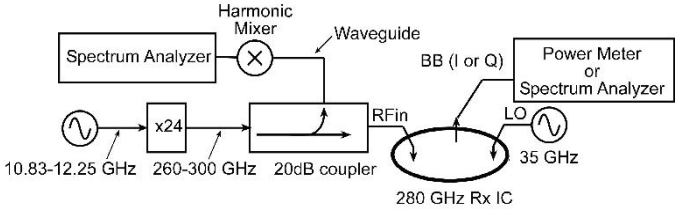

Fig. 3. Receiver continuous wave (CW) testing setup.

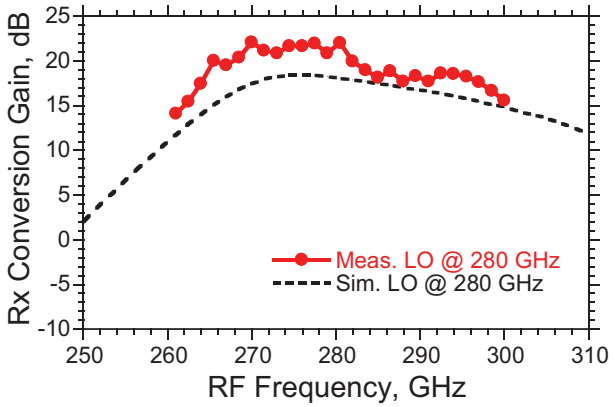

Fig. 4. Conversion gain vs. RF frequency at a fixed 280 GHz LO frequency.

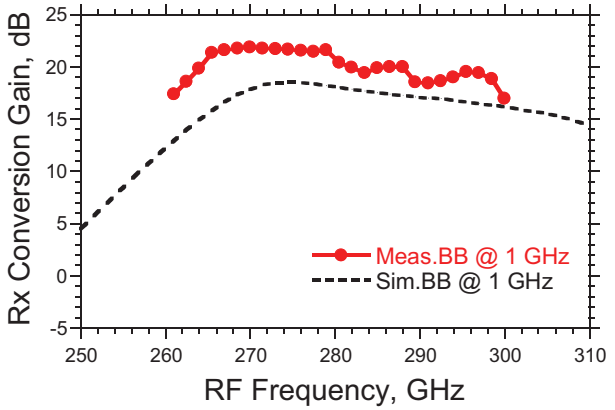

Fig. 5. Conversion gain vs. RF frequency at a fixed 1 GHz output frequency.

The input RF frequency f_{RF} was first swept with a fixed 280 GHz LO frequency (Fig. 4). The peak measured conversion gain, to a single-ended output, was 22 dB; gains using the differential outputs would be 3 dB greater. Over 260-280 GHz, the measured gain was ~2-4 dB greater than simulated; over 280-300 GHz it is ~1-2 dB greater. The measured –3 dB bandwidth is 16.5 GHz, while the measured –6 dB bandwidth is 34.5 GHz. CB amplifiers in this technology often show higher gain than simulated [10].

The RF and LO frequencies were then swept with a fixed 1 GHz baseband frequency (Fig. 5). This showed 20.4 dB measured conversion gain at 280.5 GHz and ~40 GHz LO-tuning bandwidth at the –6 dB points.

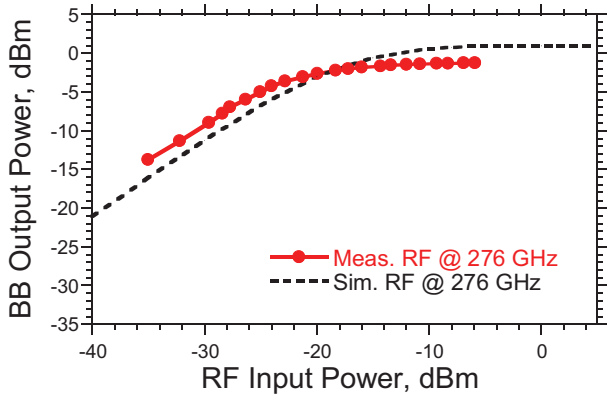

Fig. 6. Baseband output power vs. RF input power at f_{LO} = 280 GHz.

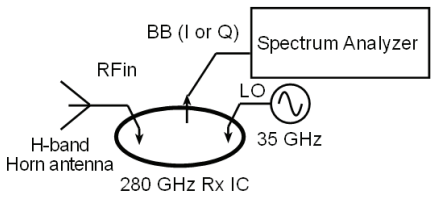

Fig. 7. Receiver noise figure measurement by the gain technique.

To measure the dynamic range, the input RF power at 276 GHz was swept while applying a 280 GHz local oscillator. P_{in1dB} is -23.6 dBm, with 455 mW dissipation (Fig. 6).

Because there is no commercially available 280 GHz hot/cold noise source, noise was instead measured by the less accurate gain method; even with the hot/cold method, measurements are difficult unless (T_{hot}–T_{cold}) is comparable to or larger than T_{DUT}. Receiver gain was first measured using the configuration of Fig. 3, with input and output powers measured using a power meter. Output noise power spectral density was then measured, at 200 MHz, using a spectrum analyzer (Fig. 7), with the RF input connected through a 220-330 GHz wafer probe to an H-band horn antenna, providing a 50 Ω, 300 K source termination. The input referred noise was determined by dividing the measured output noise by the measured receiver gain, dividing by kT, and subtracting 3 dB to convert from single sideband (SSB) to DSB noise figure. The measured receiver DSB noise figure is 10-11.6 dB over 261-300 GHz (Fig. 8). Measured noise is 1.5-2.5 dB below original design simulations. However, over 260-300 GHz, the measured receiver gain is 1-4 dB greater than that simulated. If this discrepancy between measured and simulated receiver gain were due to greater LNA gain than simulated, then the contributions to the receiver noise of the mixer and of the 2nd, 3rd and 4th LNA stages would be reduced. A simple calculation shows that the reduction of the mixer noise alone would reduce the disparity between simulation and measurement to 1-1.5 dB, even neglecting the reduced noise contributions of the 2nd-4th LNA stages. The measured DSB receiver noise (Fig. 8) is very similar to that of [15], for an LNA at the same frequency in the same technology, and similar to [16], an LNA in a similar technology, though [15,16] are LNA, not receiver results.

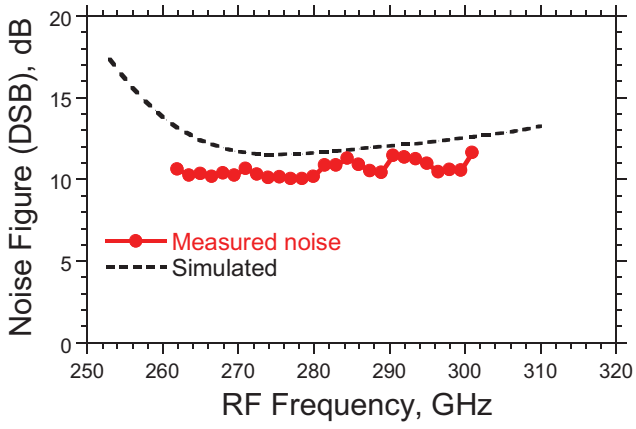

Fig. 8. Measured vs simulated receiver DSB noise figure.

Table 1. State-of-the-art receivers at above 200 GHz.

Ref	[1]	[2]	[3]	[4]	[5]	[6]	[7]	[8]	[9]	This work
Freq, GHz	240	220	220	240	240	240	200	300	340	**280**
Conversion Gain, dB	25	1.5	3.5	18	32	10.5	25	26	14	**22**
P_{DC}, mW	260	-	110	512	575	866	825	482	472	**455**
Chip Size, mm^2	2	1.5	4.8	2.1	4.5	1.56	2	1.32	3	**1.6**
DSB NF, dB	15[a]	7.5[a]	7.4	18[b]	10.4	12	8	12-16.3	17	**10.8**
Technology	65 nm CMOS	50 nm GaAs mHEMT	100 nm GaAs mHEMT	130 nm SiGe HBT	130 nm SiGe HBT	130 nm SiGe HBT	250 nm InP HBT	250 nm InP HBT	250 nm InP HBT	**250 nm InP HBT**

[a]calculated, [b]simulated

We do not believe that an on-wafer 220-330 GHz receiver noise measurement, by the gain method, can be accurate to better than approximately +/-1 dB.

IV. Conclusion

In this paper, a fully integrated 280 GHz receiver with record noise figure is presented. The peak conversion gain is 22 dB with 34.5 GHz of -6 dB modulation bandwidth with 455 mW dissipation. The measured DSB noise figure is 10.8 dB at 281.5 GHz.

Acknowledgment

This work was supported by ComSenTer, a JUMP program sponsored by the Semiconductor Research Corporation. The authors thank Teledyne Scientific & Imaging for the IC fabrication.

References

[1] S. V. Thyagarajan, S. Kang and A. M. Niknejad, "A 240 GHz Fully Integrated Wideband QPSK Receiver in 65 nm CMOS," in IEEE Journal of Solid-State Circuits, vol. 50, no. 10, pp. 2268-2280, Oct. 2015.

[2] I. Kallfass et al., "All Active MMIC-Based Wireless Communication at 220 GHz," in IEEE Transactions on Terahertz Science and Technology, vol. 1, no. 2, pp. 477-487, Nov. 2011.

[3] M. Abbasi et al., "Single-Chip 220-GHz Active Heterodyne Receiver and Transmitter MMICs With On-Chip Integrated Antenna," in IEEE Transactions on Microwave Theory and Techniques, vol. 59, no. 2, pp. 466-478, Feb. 2011.

[4] M. Elkhouly, Y. Mao, S. Glisic, C. Meliani, F. Ellinger and J. C. Scheytt, "A 240 GHz direct conversion IQ receiver in 0.13 µm SiGe BiCMOS technology," 2013 IEEE Radio Frequency Integrated Circuits Symposium (RFIC), Seattle, WA, USA, 2013, pp. 305-308.

[5] M. H. Eissa et al., "Wideband 240-GHz Transmitter and Receiver in BiCMOS Technology With 25-Gbit/s Data Rate," in IEEE Journal of Solid-State Circuits, vol. 53, no. 9, pp. 2532-2542, Sept. 2018.

[6] N. Sarmah et al., "A Fully Integrated 240-GHz Direct-Conversion Quadrature Transmitter and Receiver Chipset in SiGe Technology," in IEEE Transactions on Microwave Theory and Techniques, vol. 64, no. 2, pp. 562-574, Feb. 2016.

[7] M. Seo, A. S. H. Ahmed, U. Soylu, A. Farid, Y. Na and M. Rodwell, "A 200 GHz InP HBT Direct-Conversion LO-Phase-Shifted Transmitter/Receiver with 15 dBm Output Power," 2021 IEEE MTT-S International Microwave Symposium (IMS), Atlanta, GA, USA, 2021, pp. 378-381.

[8] S. Kim et al., "300 GHz Integrated Heterodyne Receiver and Transmitter With On-Chip Fundamental Local Oscillator and Mixers," in IEEE Transactions on Terahertz Science and Technology, vol. 5, no. 1, pp. 92-101, Jan. 2015.

[9] Y. Yan, Y. B. Karandikar, S. E. Gunnarsson, M. Urteaga, R. Pierson and H. Zirath, "340 GHz Integrated Receiver in 250 nm InP DHBT Technology," in IEEE Transactions on Terahertz Science and Technology, vol. 2, no. 3, pp. 306-314, May 2012.

[10] M. Urteaga, Z. Griffith, M. Seo, J. Hacker and M. J. W. Rodwell, "InP HBT Technologies for THz Integrated Circuits," in Proceedings of the IEEE, vol. 105, no. 6, pp. 1051-1067, June 2017.

[11] U. Soylu, A. Alizadeh, M. Seo and M. J. W. Rodwell, "A 280 GHz (x8) Frequency Multiplier Chain in 250 nm InP HBT Technology," 2022 IEEE BiCMOS and Compound Semiconductor Integrated Circuits and Technology Symposium (BCICTS), Phoenix, AZ, USA, 2022, pp. 191-194.

[12] A. S. H. Ahmed, A. A. Farid, M. Urteaga and M. J. W. Rodwell, "204GHz Stacked-Power Amplifiers Designed by a Novel Two-Port Technique," 2018 European Microwave Integrated Circuits Conference (EuMIC), Madrid, 2018, 23-25 Sept. 2018

[13] A. S. H. Amed, M. Seo, A. Farid, M. Urteaga, J. Buckwalter, M. Rodwell, "A 140GHz power amplifier with 20.5dBm output power and 20.8% PAE in 250-nm InP HBT technology" 2020 IEEE International Microwave Symposium, June 21-26, Los Angeles, CA

[14] U. Soylu, A. S. H. Ahmed, M. Seo, A. Farid and M. Rodwell, "200 GHz Low Noise Amplifiers in 250 nm InP HBT Technology," 2021 16th European Microwave Integrated Circuits Conference (EuMIC), London, United Kingdom, 2022, pp. 129-132.

[15] K. Eriksson, S. E. Gunnarsson, V. Vassilev and H. Zirath, "Design and Characterization of H-Band (220–325 GHz) Amplifiers in a 250-nm InP DHBT Technology," in IEEE Transactions on Terahertz Science and Technology, vol. 4, no. 1, pp. 56-64, Jan. 2014.

[16] H. -J. Song and M. Yaita, "On-Wafer Noise Measurement at 300 GHz Using UTC-PD as Noise Source," in IEEE Microwave and Wireless Components Letters, vol. 24, no. 8, pp. 578-580, Aug. 2014.